Water Resources Management (2021) 35:2649–2666
https://doi.org/10.1007/s11269-021-02857-9

Estimation of the Interaction Between Groundwater and Surface Water Based on Flow Routing Using an Improved Nonlinear Muskingum-Cunge Method

Chengpeng Lu[1] · Keyan Ji[1] · Wanjie Wang[1] · Yong Zhang[2] · Tema Koketso Ealotswe[1] · Wei Qin[1] · Jiayun Lu[1] · Bo Liu[1] · Longcang Shu[1]

Received: 3 February 2021 / Accepted: 17 May 2021/ Published online: 27 May 2021
© The Author(s), under exclusive licence to Springer Nature B.V. 2021

Abstract
The interaction between groundwater (GW) and surface water (SW) not only sustains runoff in dry seasons but also plays an important role in river floods. Lateral inflow is the recharge of groundwater to surface water during a river flood; this recharge is part of the GW-SW exchange. Hydrological engineers proposed the idea of modelling flood routing using the Muskingum-Cunge method, in which the GW-SW exchange is not fully considered. This study proposes an improved nonlinear Muskingum-Cunge flood routing model that considers lateral inflow; the new method is denoted as NMCL1 and NMCL2 and can simulate flood routing and calculate the GW-SW exchange. In addition, both the linear and nonlinear lateral inflows (with the channel inflows) are discussed, and the stable lateral inflows that occur due to the GW-SW exchange are considered for the first time. A sensitivity analysis shows that different parameters have different effects on the simulation results. Three different flood cases documented in the literature are selected to compare the four classical and two updated Muskingum-Cunge methods. Two different floods of the River Wye are selected to verify the accuracy of the calibrated model. The simulation results of the improved Muskingum-Cunge method are compared with the temperature inversion results measured from the Zhongtian River, China, to indicate the feasibility and reliability of the improved method. A comparison shows that, for several cases, the proposed method is capable of obtaining optimal simulation results. The proposed method inherits the ability of the Maskingum-Cunge method to simulate flood routing. Moreover, it can quantify the GW-SW exchange, and the reliability of the estimations is owed to the nonlinearity and sign flexibility of the calculated exchange process.

Keywords Muskingum flood routing · Lateral inflow · Interaction of groundwater and surface water · Parameter sensitivity analysis · Field investigations

✉ Chengpeng Lu
luchengpeng@hhu.edu.cn

✉ Yong Zhang
yzhang264@ua.edu

Extended author information available on the last page of the article

1 Introduction

Groundwater (GW) and surface water (SW) are two components of hydrologic systems that exist in mountain rock strata, river systems, and coastal and karst terrain environments. These elements must be considered in calculations of the hydrological cycle and water budget, which interact at various spatiotemporal scales and regulate ecological and biogeochemical processes (Krause et al. 2011; Shuai et al. 2017;). Groundwater is the dominant factor of the hydrological cycle and water resource transformations in some basins, especially for ecological vegetation in some arid areas. In areas with scarce precipitation, leakage from riverbeds accounts for a large proportion of groundwater recharge. In the dry season, groundwater aquifers discharge into rivers in the form of base flow to ensure the flow of rivers and maintain ecosystems (Hussein and Schwartz 2003). Considering the GW-SW interaction and revealing the evolutionary characteristics of the water cycle are important components of scientific water resource management (Werner et al. 2006). It is of critical importance to quantify the GW-SW interaction to maintain river ecosystems and manage water resources (Welch et al. 2013). Direct measurement methods are limited to homogeneous and simplified boundary areas, and it is difficult to obtain long-scale data. Geological and hydrological conditions differ among different basins, and these conditions are complex and have great uncertainty under specific hydrological events (Ahiablame et al. 2013). Temperature tracing and hydrochemical methods can be used to analyse the recharge and discharge relationships between groundwater and surface water, but it is difficult to describe the spatiotemporal variations in the GW-SW interaction using these methods (Schmidt et al. 2006). In addition, base flow segmentation is also a common method used to study river groundwater (Moon et al. 2004), but it cannot estimate the contribution of surface water to groundwater during a flood. Some groundwater-surface water coupled models, such as MODFLOW and GSFLOW, can simulate routing and estimate exchange capacity at the same time (Werner et al. 2006; Tran et al. 2020). However, coupled models are more computationally intensive and have high data demands and great uncertainty. Ensuring accuracy and improving simplicity simultaneously when quantifying the interaction of GW-SW motivate the carrying out of this study.

This study tries to evaluate the GW-SW exchange in lumped flow routing, a classical hydrological procedure to obtain a flow hydrograph. This is the case for the well-known Muskingum-Cunge (MC) model (Cunge 1969). To realistically simulate the nonlinear processes of flood movements in rivers, models such as the Muskingum method are modified to account for the nonlinearity of flow movement processes (Karahan et al. 2013; Niazkar and Afzali 2015). Gill (1978) first introduced a nonlinear storage equation using the exponent of the Muskingum storage equation as the third parameter.

Unfortunately, traditional models ignore the fact that lateral flow exists in river reaches in actual flood events. The lateral flow that occurs during flooding may be either inflow or outflow. Outflow refers to the loss of surface water through porous riverbeds and river embankments. Inflow refers to the lateral flow into a river that is contributed by rainfall in the catchment. Ignoring the lateral flow will lead to a large deviation between the simulated flood wave and the measured flood wave. To overcome this apparent limitation, state-of-the-art MC models with multiple parameters and lateral flow have been developed by several researchers. For example, Ayvaz and Gurarslan (2017) and Kang et al. (2017) considered lateral inflow in the MC method. Barbetta et al. (2017) extended the variable-parameter Muskingum stage hydrograph routing method.

Although lateral inflow has been considered in hydrological modelling, the GW-SW exchange is still ignored. This is not in line with the actual situation. First, lateral inflow was assumed to be linearly related to the channel inflow (Ayvaz and Gurarslan 2017; Karahan et al. 2015). This assumption is only feasible when considering the slope flow between sections. Affected by unsteady precipitation and complex aquifer heterogeneity, GW level dynamics tend to exhibit nonlinear and heterogeneous characteristics. Second, there is no constant term for the slope flow assumption. The exchange between GW and SW is primarily controlled by the water level difference between them; therefore, in most cases, the interaction is not zero even when the river inflow is zero.

The purpose of this study is mainly divided into two parts: to further explore the influence of parameters on the Muskingum model and to estimate the GW-SW exchange while simulating flood routing to prevent groundwater floods. The nonlinear water exchange term is added in the improved model, allowing the physical routing of river floods to be more reasonable. In the actual simulation, flood routing (peak discharge, etc.) can be more accurately simulated and predicted, while a reasonable estimation of the river water and groundwater exchange capacity can be obtained simultaneously. The improved model can prevent groundwater flooding in extreme flood events and has practical significance in groundwater management and flood control.

2 Methodology Development

2.1 MC Models

2.1.1 MC Models without Lateral Flow (MC1, MC2, and NMC1)

The conventional MC method is based on channel storage and the water balance equation (Geem 2006; Gill 1978). The earliest linear Muskingum channel storage equation assumed that the storage, S, of a reach is linearly related to the flow, Q:

$$S = K[XI + (1-x)\mathrm{Q}] \tag{1}$$

where x represents the relative proportion of the influence of inflow and outflow on channel storage. The terms K and x are determined according to the channel and flood characteristics. The water balance equation and the storage equation are decomposed in the temporal domain, and the following flow routing equation can be obtained (named MC1):

$$Q_t = C_0 I_t + C_1 I_{t-1} + C_2 Q_{t-1} \tag{2}$$

where C_0, C_1 and C_2 are functions of the Muskingum method with respect to parameters K and x, the sum of which is equal to 1. While the time step (Δt) is set, the three coefficients can be obtained using the equations recommended by O'Donnell (1985).

Cunge (1969) proved that the Muskingum method is a second-order approximate solution of diffusion waves. He connected the Muskingum method with diffusion waves in hydraulics and proposed the Muskingum-Cunge (MC) method. For a certain reach, the method first gives a single wide reference flow, estimates the wave velocity and hydraulic diffusivity in the

diffusion wave equation, and then, as a constant, uses the difference scheme to solve the motion wave equation. In the MC version, K and x are calculated using the following formulas derived by Cunge (1969) (named MC2):

$$K = \frac{\Delta x}{c} \tag{3}$$

$$x = \frac{1}{2}\left(1 - \frac{I}{c \cdot S \cdot \Delta x}\right) \tag{4}$$

in which Δx represents the reach length (i.e., the space interval), c is the flood wave celerity, I is the unit width discharge, and S is the channel bed slope.

Both the Muskingum method (MC1) and the Muskingum-Cunge method (MC2) assume a linear relationship between flow and storage (Moghaddam et al. 2016). This assumption is not valid for some river reaches, especially in the middle and lower reaches of large and medium riverbeds, where the slope of the river is small and the flow velocity increases rapidly with an increase in the water level; this nonlinearity motivated the establishment of nonlinear Muskingum models (Mohan 1997), such as the following nonlinear Maskingum method (named NMC1) proposed by Gill (1978):

$$S_t = K[xI_t + (1-x)Q_t]^m \tag{5}$$

$$Q_t = \frac{1}{1-x}\left(\frac{S_t}{K}\right)^{\frac{1}{m}} - \frac{x}{1-x} \cdot I_t \tag{6}$$

where the new parameter m is the exponent of the power-law relationship between the accumulated storage and the weighted flow. When $m = 1$, Eq. (5) is reduced to the specific linear relation.

2.1.2 MC Models with Lateral Flow (MCL1)

All the models mentioned above ignore the lateral flow that exists in the river reaches during actual flood events. O'Donnell (1985) assumed that the lateral flow entering a river reach was directly proportional to the inflow, with a proportionality factor β, and then proposed the first MC model with lateral flow.

$$\frac{dS_t}{dt} = (1+\beta)I_t - Q_t \tag{7}$$

$$S_t = K[(1+\beta)xI_t + (1-x)Q_t] \tag{8}$$

$$Q_{lat} = \beta I \tag{9}$$

Integrating the nonlinear continuity and storage equations that take lateral flow into consideration, one obtains the following equations.

$$S_t = K[(1+\beta)xI_t + (1-x)Q_t]^m \tag{10}$$

$$Q_t = \frac{1}{1-x}\left(\frac{S_t}{K}\right)^{\frac{1}{m}} - \frac{x(1+\beta)}{1-x}I_t \tag{11}$$

Tung (1985) and Geem (2006) suggested using the inflow at the previous time step (I_{t-1}) rather than at the current time (I_t) when calculating the outflow (Q_t). Geem (2006) discussed this issue and confirmed that under optimal parameter conditions, when calculating Q_t, I_{t-1} is better than I_t (named MCL1).

$$Q_t = \frac{1}{1-x}\left(\frac{S_t}{K}\right)^{\frac{1}{m}} - \frac{x(1+\beta)}{1-x}I_{t-1} \tag{12}$$

2.2 Improved MC Method to Calculate the GW-SW Interaction (NMCL1 and NMCL2)

The MC methods reviewed above assume that the lateral inflow is linearly proportional to the inflow. A zero-value inflow leads to zero lateral inflow, and this relationship cannot explain the potential lateral inflow that occurs due to the GW-SW interaction. To solve this issue, it is hereby first assumed that a stable GW-SW interaction process exists before a flood event, and a constant representing the stable exchange volume in the storage is added (named NMCL1):

$$S_t = K[(1+\beta)xI_t + (1-x)Q_t + e]^m \tag{13}$$

where e represents the stable lateral inflow due to the GW-SW exchange. We can then estimate the sum of the GW-SW interaction and lateral inflow using the following equation.

$$Q_{lat} = I_t\beta + e \tag{14}$$

Another option is to consider the nonlinear relationship between the lateral inflow and the channel inflow, leading to the following storage equation (named NMCL2):

$$S_t = K\left[xI_t + (1-x)Q_t + e + {I_t}^{\beta}\right]^m \tag{15}$$

where β no longer represents the ratio coefficient of lateral inflow, but instead represents the power exponent. The sum of the vertical inflow that occurs due to the GW-SW interaction and the transient lateral inflow can be calculated as folows:

$$Q_{lat} = {I_t}^{\beta} + e \tag{16}$$

The sum of the squared errors (SSQ), the Nash efficiency coefficient (NSE), and the root mean square error (RMSE) are used as the objective functions.

The calculated S_{t+1} and Q_{t+1} values may induce negative or complex values for the generated parameters K, x, and m (Karahan et al. 2013). To solve this problem, the following penalty functions are used:

$$S^*_{t+1} = \begin{cases} S_{t+1} & if\ \ S_{t+1} \geq 0 \\ \lambda_1 |S_{t+1}| & if\ \ S_{t+1} < 0 \\ \lambda_1 |RS_{t+1}| & if\ \ S_{t+1}\ \ is\ \ complex \end{cases} \tag{17}$$

$$Q_{t+1}^{*}=\begin{cases} Q_{t+1} & if\ \ Q_{t+1}\geq 0 \\ \lambda_2\left|Q_{t+1}\right| & if\ \ Q_{t+1}<0 \\ \lambda_2\left|RQ_{t+1}\right| & if\ \ Q_{t+1}\ \ is\ \ complex \end{cases} \tag{18}$$

where λ_1 and λ_2 are the penalty constants and $R(\cdot)$ is the real part of the complex numbers S_{t+1} and Q_{t+1}. The equations above state that if S_{t+1} or Q_{t+1} is less than zero, S_{t+1}^{*} or Q_{t+1}^{*} is then used in the routing procedure. Note that the two constants λ_1 and λ_2 can be case-dependent. Preliminary tests are needed the actual search process to determine λ_1 and $\lambda_2$can be started.

The particle swarm optimization (PSO) approach, an intelligent cluster optimization algorithm (Eberhart and Kennedy 1995), was applied for parameter optimization. The comprehensive sensitivity was calculated according to the equations proposed by Kabala (2001) and Doherty (2004).

In summary, MC1, MC2, and NMC1 are traditional MC models that do not consider lateral flow. The NMC1 method assumes a nonlinear relationship between the accumulated storage and the weighted flow. On this basis, the MCL1 method was proposed, considering the lateral inflow. In this paper, the MCL1 method was further improved to obtain the NMCL1 and NMCL2 methods; these methods were proposed to estimate the GW-SW exchange during floods. The conceptual model of the study is shown in Fig. 1. Three types of flood cases were selected from the literature denoted as Wilson (1974), O'Donnell (1985), and Viessman and Lewis (2003). Using the optimal parameters, the results of three cases simulated by six MC methods were compared.

3 Model Validation

3.1 Sensitivity Analysis of MC Parameters

The parameter sensitivity analysis was performed by adjusting the five parameters (Table 1). We chose the NMCL1 and NMCL2 methods.

The observed flow at the River Wyre in the UK from O'Donnell (1985) was selected here for the sensitivity analysis. This example involves an inflow with multi peaks. A significant amount of lateral flow resulted in the observed outflow being far greater than the inflow. The optimal solution vectors were obtained using the PSO algorithm (Table 2). The results of the error analysis of the flood routing simulation are shown in Table 3.

In the sensitivity analysis, the bounds for the five parameters *x, k, m, e,* and β in NMCL1 and NMCL2 and the sensitivity of each parameter are shown in Table 1. The results are shown in Fig. 2.

Figure 2a–e shows the flood processes simulated by adjusting *x*, *K*, *m*, *e* and β. Figure 2a1, a2 shows that the model solution is more sensitive to parameter *x* than to the other parameters, considering that the largest fluctuation of model results was obtained by adjusting *x*. A larger *x* causes a larger fluctuation and more irregularity in the modelled outflow. A larger *x* (>0) indicates more storage for the wedge, so that more river inflow (from the channel) can directly transfer to outflow, resulting in stronger outflow fluctuations, especially during the advance of a flood event.

The simulation results are sensitive to changes in *K* (Fig. 2b1, b2). A larger *K* generates a smoother outflow curve with a lower flood peak. According to Table 1, the sensitivity of parameter *K* is small. The *K* parameter can be viewed as the lag or travel time through a river

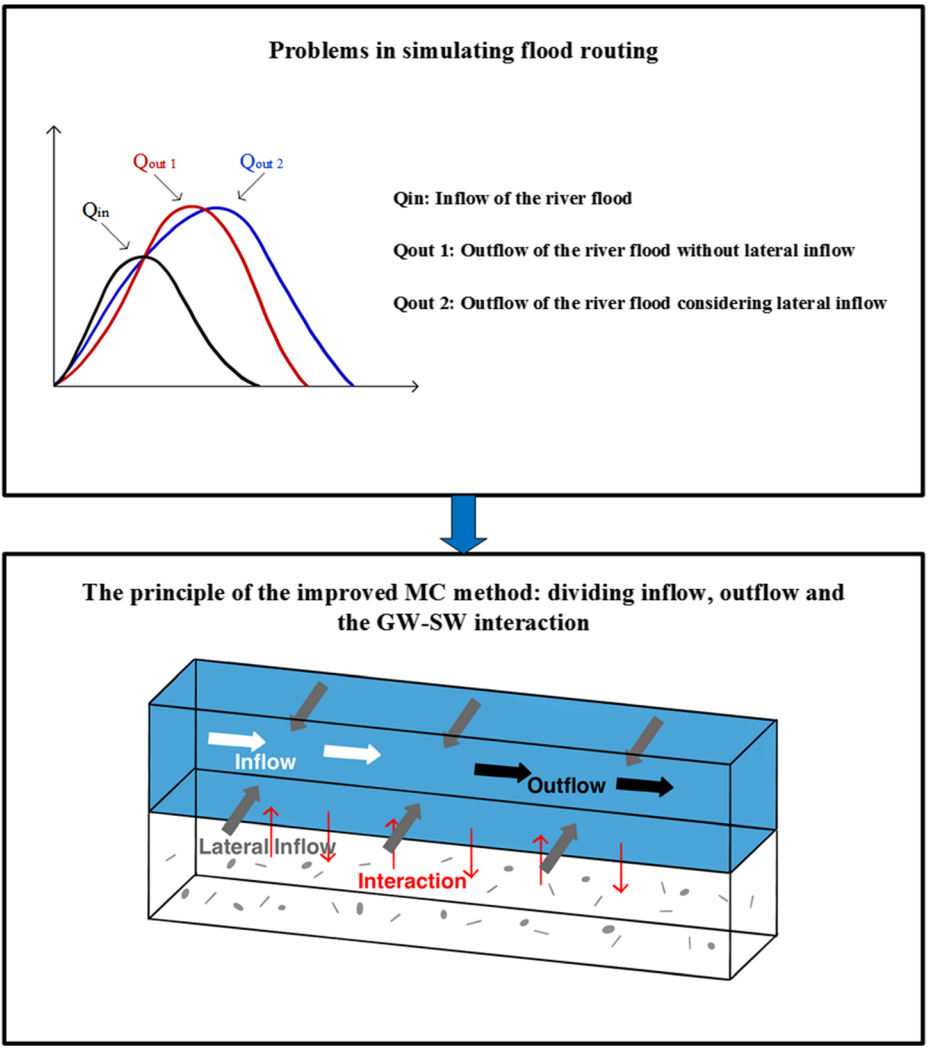

Fig. 1 The upper figure shows the limitations of the traditional Muskingum method. In a real river channel, there is always lateral inflow during a flood event. When simulating the outflow hydrograph according to the inflow, neglecting this lateral inflow may result in large errors. The lower figure shows the innovation of this study. The interaction of GW and SW plays an important role in river floods. Lateral inflow is a part of the GW-SW exchange. In this paper, the exchange volume is estimated while simultaneously using the MC method to simulate the flood process

reach (Karahan 2012). When K is smaller, the difference between the rise and fall of a flood in the reach is larger, and the water storage capacity of the channel is also reduced. When K is equal to 1, the channel water storage is very small and the flood fluctuation increases. At this time, the outflow needs to be increased to balance the water storage of the river, leading to the amplification of the outflow and the increase of the fluctuation.

The parameter m is an index in Eqs. (13) and (15) and affects the flood simulation results (Fig. 2c). According to Table 1, m shows the largest impact on the outflow. To further reveal the influence of parameter m on the simulation results, m=0.7 is added to the picture. When m decreases to 0.7, the simulated flow process also exhibits apparent fluctuations.

Table 1 The simulation ranges and sensitivities of different parameters used in the two methods

Method	NMCL1					NMCL2				
Parameter	x	K	m	e	β	x	K	m	e	β
Unit	*	h	*	m^3/s	*	*	h	*	m^3/s	*
Range	0.9~0.9	15~35	0.92~1.12	0~10	1.35~3.35	−0.9~0.9	1~21	0.92~1.12	2.3~12.3	1.04~1.44
Sensitivity for Outflow	63,962	1453	150,316	376	2081	106,468	7329	149,125	175	33,077
Sensitivity for Interaction	\	\	\	227	6673	\	\	\	254	56,432

The contents in brackets represent the units, "*" represents a dimensionless unit, and "\" represents inapplicability for the corresponding sensitivity

The sensitivity of parameter e to the simulated outflow, as shown in Fig. 2d, f and in Table 1, is the smallest. The change in parameter e is equal to the change in the exchange volume, indicating that a change in the stable lateral inflow causes the same change in the exchange volume, i.e., $\Delta EX = \Delta e$. The change in this parameter is similar to that of the simulated outflow, i.e., $\Delta Q_{out} = \frac{\Delta e}{1-x}$.

As shown in Fig. 2e, g and in Table 1, the outflow is more sensitive to parameter β than to parameter e. This sensitivity is higher for the NMCL2 method than for the NMCL1 method. This discrepancy may be due to the different roles of β in the two methods: β is an index in NMCL2 (15), while it is a multiplier in NMCL1 (13). A smaller β value leads to a smoother flood curve with a smaller outflow.

In general, m is the most sensitive parameter and has the greatest impact on the simulated outflow and routing shape. When this parameter is small enough, it also has a large impact on the simulation results. The influence of a change in parameter x on the results is second only to

Table 2 The six Muskingum-Cunge methods are simulated by the PSO algorithm 10,000 times to obtain the optimal parameters

Datasets	Parameter	MC1	MC2	NMC1	MCL1	NMCL1	NMCL2
Wilsom [1974]	x	0.221	0.385	0.187	0.247	0.258	0.236
	K	29.165	3.492	0.080	0.335	0.251	0.425
	m	\	\	2.283	1.948	2.005	1.901
	β	\	\	\	−0.023	−0.045	−0.293
	e	\	\	\		1.199	−1.467
O'Donnell [1985]	x	0.771	−0.086	0.756	0.170	0.213	−0.886
	K	6.957	0.870	19.987	24.894	24.645	10.769
	m	\	\	5.417	1.031	1.026	1.022
	β	\	\	\	2.541	2.349	1.243
	e	\	\	\		3.168	7.323
Viessmn and Lewis [2003]	x	0.187	2.223	−0.009	0.094	0.106	0.092
	K	12.094	8.230	0.220	0.287	0.199	0.270
	m	\	\	1.533	1.496	1.541	1.504
	β	\	\	\	−0.003	−0.025	−0.327
	e	\	\	\		20.657	2.652
Two floods at River Wye	x	0.278	3.172	0.223	0.304	0.316	0.314
	K	24.039	3.829	0.009	0.147	0.098	0.094
	m	\	\	2.169	1.727	1.784	1.787
	β	\	\	\	0.049	0.014	0.401
	e	\	\	\		13.110	8.150

Table 3 Three error objective functions obtained using six MC methods in three cases of flooding

Datasets	Objective function	MC1	MC2	NMC1	MCL1	NMCL1	NMCL2
Wilson [1974]	SSQ(m^6/s^2)	605.63	448.45	178.98	19.59	17.55	24.11
	NSE(*)	0.9504	0.9633	0.9854	0.9984	0.9986	0.9980
	RMSE(m^3/s)	5.247	4.515	2.852	0.944	0.893	1.047
O'Donnell [1985]	SSQ(m^6/s^2)	50,686.00	13,618.00	29,043.00	122.09	98.01	125.13
	NSE(*)	−0.7425	0.5318	0.0015	0.9958	0.9966	0.9957
	RMSE(m^3/s)	39.799	20.629	30.126	1.953	1.750	1.977
Viessman and Lewis [2003]	SSQ(m^6/s^2)	124,310.00	110,620.00	82,227.00	73,811.00	71,708.00	73,774.00
	NSE(*)	0.9714	0.9745	0.9811	0.9830	0.9835	0.9830
	RMSE(m^3/s)	71.969	67.891	58.533	55.457	54.661	55.443

The contents in brackets represent units, while "*" represents a dimensionless unit

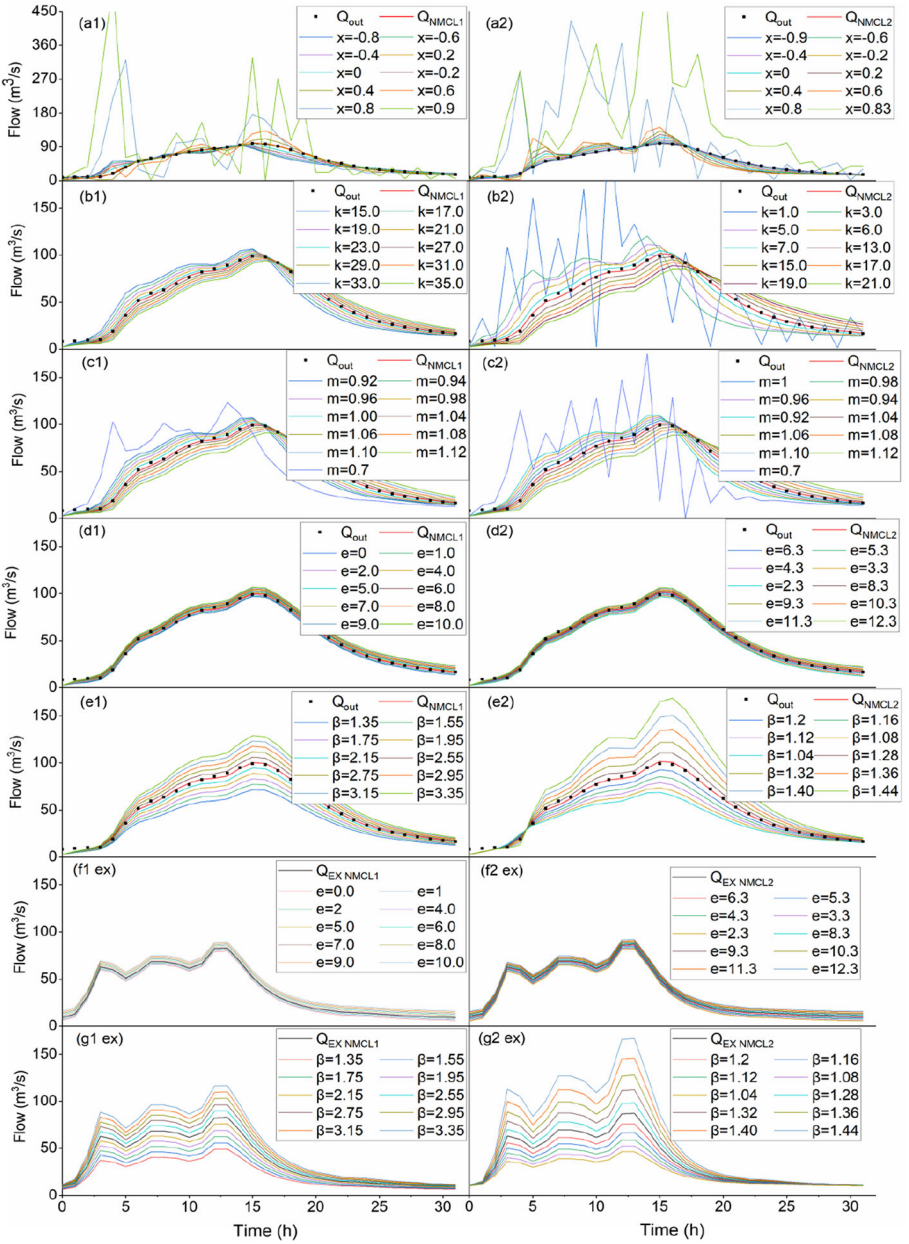

Fig. 2 Results of the parameter sensitivity analysis. Q_{out} is the measured outflow. Q_{NMCL1} and Q_{NMCL2} are the best-fit outflows with optimized parameters, and Q_{EX} represents the sum of the transient/conventional lateral inflow and the stable inflow/vertical inflow due to the GW-SW exchange. Panels (**a**–**e**) represent the influences of parameters x, K, m, e and β on the modelled outflow, respectively. Panels (**f**–**g**) represent the influences of parameters e and β on the estimated exchange volume between GW and SW, respectively. The numbers in the upper left corner of each figure "1" and "2" represent the NMCL1 and NMCL2 methods, respectively

that of parameter m. The parameter e is the least sensitive parameter, and the influence of this parameter on the simulation results is equal.

3.2 Validation Via Published Data

Six methods were used to simulate the three cases. Table 3 lists the error analysis of the flood routing simulation results.

3.2.1 Flow Data from Wilson (1974)

The first example (Wilson 1974) was a smooth single-peak hydrograph with a low lateral flow contribution. We used the six MC methods mentioned above to simulate flood routing in Wilson's data.

The results obtained after running the PSO algorithm 10,000 times to estimate the optimal parameters are shown in Table 2. As listed in Table 3, the simulation results of the conventional MC1 and MC2 methods poorly match the data. The best-fit models are MCL1 and NMCL1.

Figure 3a1, a2 shows that all six methods can capture the overall shape of the observed flood routing. During this flood event, the GW and SW exchange was very small. The values estimated by MCL1 and NMCL2 were similar and negative (i.e., recharge to groundwater). The value estimated by the NMCL1 method was positive at the beginning of the flood event and then became negative.

3.2.2 Flow Data from O'Donnell (1985)

The flood data observed at the River Wyre, UK (O'Donnell 1985) have considerable lateral inflow. We use the six MC methods mentioned above to simulate flood routing.

The best-fit parameters are shown in Table 2. Table 3 confirms that the conventional methods, which ignore the lateral inflow, failed to simulate flood routing. The solution of NMCL1 matched the data best, with a relatively low SSQ (98).

Figure 3b1–2 shows that the first three conventional MC methods (MC1, MC2, and NMC1) failed to simulate the flood routing process, and MCL1, NMCL1 and NMCL2 fit well with the observed outflow hydrograph.

The simulated GW-SW exchange was larger than the river inflow, and all the values were positive, implying that the surface water gained more water from groundwater than it lost.

3.2.3 Flow Data from Viessman and Lewis (2003)

Viessman and Lewis (2003) observed a flow hydrograph with two peaks. The optimal parameters are shown in Table 2. The resultant error are listed in Table 3. The two conventional MC methods had the largest errors. The best method was NMCL1.

Figure 3c1, c2 shows that the flood hydrographs simulated by the six methods are generally consistent with the shape of the observed outflow. In the transition period between the two flood peaks, the error between the simulation results and the observation is large. In the Muskingum method, it is considered that there is a direct corresponding relationship between the channel storage and the linear combination of inflow and outflow, representing a single flood in an actual channel. Therefore, in the routing simulation of this case, the error of the simulation results between two flood peaks is large. This dataset implies low contributions of the lateral inflow and the exchange of GW-SW to the outflow.

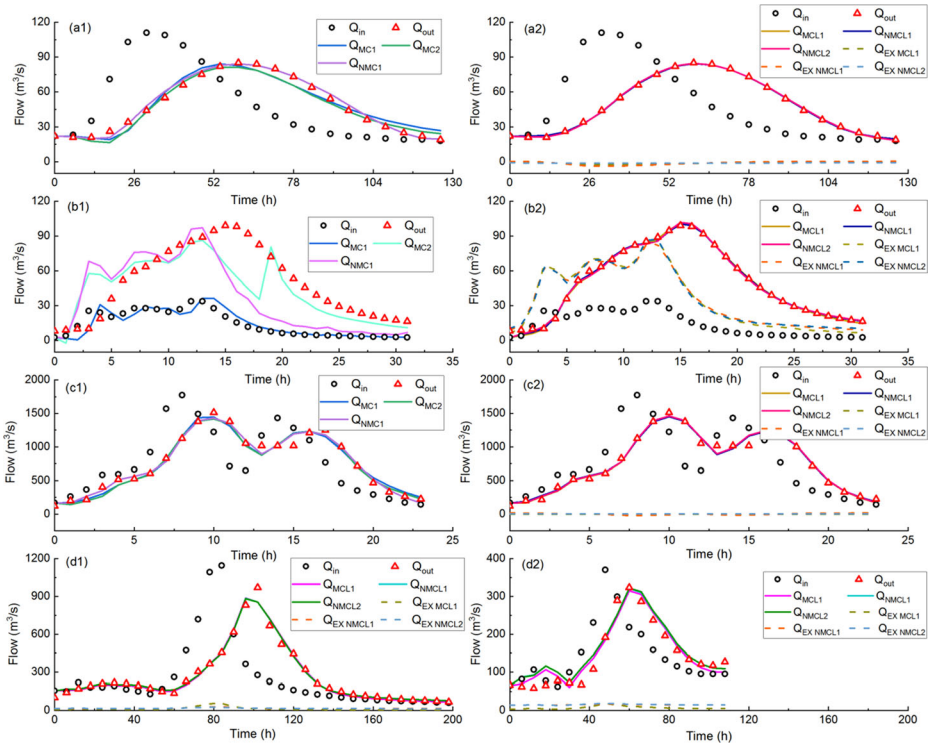

Fig. 3 The measured versus modelled results of the flow data obtained from the literature. Picture (**a1**, **a2**) show the results for Wilson (1974), (**b1**, **b2**) are for O'Donnell (1985) and (**c1**, **c2**) are for Viessman and Lewis (2003). Panels (**d1**, **d2**) show the two different flow datasets of the River Wye from O'Donnell (1985). The left figure shows the simulation results of the traditional Muskingum method, and the right figure shows the simulation results of the improved method. Q_{in} and Q_{out} are the measured inflow and outflow values, respectively. Q_{MC1} is the outflow estimated using MCL1, Q_{MC2} is the outflow estimated using MC2, Q_{NMC1} is the outflow estimated using NMC1, Q_{MCL1} is the outflow estimated using MCL1, Q_{NMCL1} is the outflow estimated using NMCL1, and Q_{NMCL2} is the outflow estimated using NMCL2. Q_{EX} represents the sum of the transient/conventional lateral inflow and the vertical inflow due to the interaction between GW and SW

3.3 Validation Using Two Different Floods in the Same River

To further verify the calibrated model, two different floods in the same river were selected for simulation. The two flood datasets were observed at the River Wye, UK (O'Donnell 1985). We use the three improved MC methods mentioned above to simulate the flood routing. The duration of one flood was 198 h, and the peak value of the outflow was 969 m^3/s; the corresponding values for the other flood are 108 h and 323 m^3/s. First, we selected the flood with the longer duration for the optimal parameter calibration and substituted the calibrated parameters to simulate the other flood. Flood 1 represents a flood duration of 198 h, and flood 2 represents a flood duration of 108 h.

The optimal parameters were estimated according to the data of flood 1, as shown in Table 2.

By analysing the errors of the simulation results, the MCL1, NMCL1 and NMCL2 methods were confirmed to successfully simulate the flood process. The simulation results of these three methodswere very close, and the simulation results of flood 1 were better than those of flood 2.

Figure 3d1, d2 shows that all three methods can capture the overall shape of the observed flood routing. The hydrographs simulated in flood 1 almost overlap. The simulation results of the flood 2 hydrograph were not as good as those of flood 1. During this flood event, the sum of the GW and SW exchange was small. The exchange volumes estimated by the three methods were all positive, indicating that the river was recharged by groundwater during the flood events.

The results mentioned above confirmed that the new method proposed in this paper can be applied to different flood simulations of the same river. Although there were differences in the sesults between the two flood simulations, the simulation results are reliable (NSE >0.9).

4 Applications

4.1 Field Investigation of the GW-SW Interaction at the Zhongtian River, China

The Zhongtian River is a second-order stream in Jiangsu Province, southeast China. The annual average temperature is 17.5 °C, and the annual rainfall is 1149.7 mm. The selected river reach is approximately 30 m long and 10 m wide. Two Levelogger Edge data loggers (3001, Solinst) were used to monitor the river stages at upstream and downstream locations. Because the real-time measured flow was not obtained, the continuously observed river stage was utilized in the MC routing based on the assumption of a linear relationship between the river stage and discharge.

The setting of the river section is shown in Fig. 1 of Lu et al. 2020. The hydrodynamic and thermal conditions in the river, groundwater, and hyporheic zone were continuously recorded and analysed for ten days from 11/23/2014 to 12/02/2014. Three rainfall events with magnitudes of 89 mm, 9 mm, and 9 mm were observed on Nov. 23–25, Nov. 27, and Nov. 29–30, respectively.

One-dimensional analytical solutions for heat transport can be used to estimate the hyporheic flow when the flow has a vertical component. We tried three popular methods, including the amplitude ratio (Ar) approach, the phase shift ($\Delta\varphi$) approach, and the combination of Ar and$\Delta\varphi$, and found that these three methods generated deviating results: we attributed these variations to the sensitivity of the Ar method to non-ideal input data (see Hatch et al. (2006)). Therefore, we chose to use the Ar method because of its robustness and consistent results.

The water flux was calculated at each of the thermal monitoring points by VFLUX, and the fluxes at the cross section (S1 to S4, from upstream to downstream) obtained by the weighted point flux results are shown in Fig. 4a. The rates of the water flux change at S1 and S4 were the largest, and the flux across S1 changed from small upward flow to larger downward flow, from -2×10^{-6} m/s to 5×10^{-6} m/s (negative and positive values represent upward and downward flows, respectively), while the flux at S4 changed from a larger upward flux to a smaller upward flux, from -7×10^{-6} m/s to 1×10^{-6} m/s. The temporal changes in flow direction along the four downstream sections first started at S1 and finished at S4. Hence, the upstream section responded to rainfall rapidly with the largest rate of change and the earliest downward flux. In the initial stage, the surface water gained water from the groundwater. Due to rainfall, the amount of water gained from groundwater decreased gradually. The flux direction at S1 upstream changed rapidly from upward flow to downward flow; meanwhile, the surface water lost water and recharged the groundwater, and the amount of supply increased gradually. Later

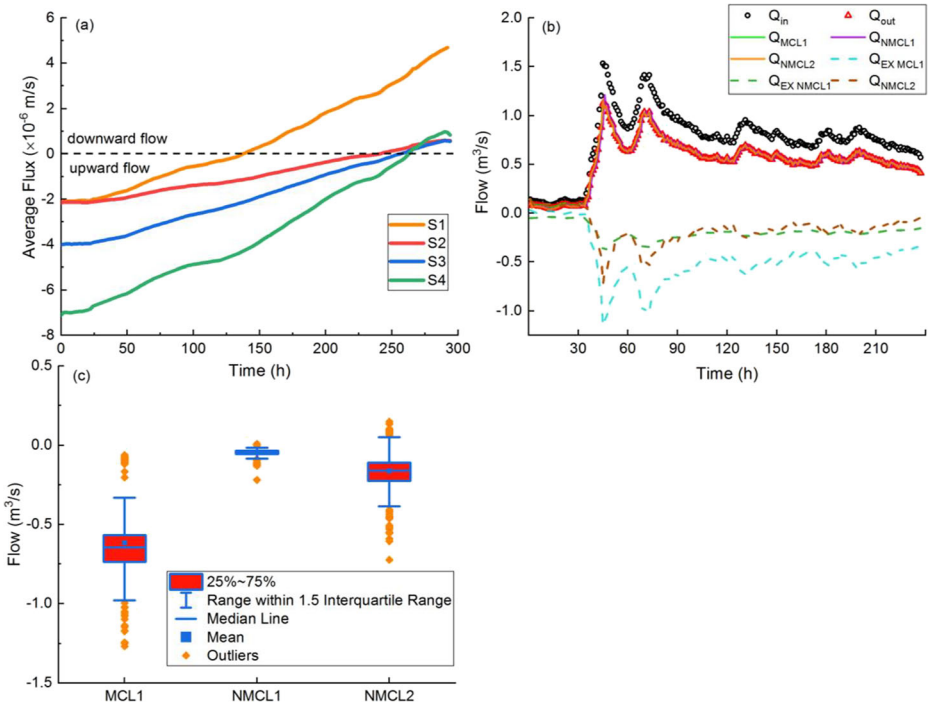

Fig. 4 Figure **a** shows the fluxes across the four cross sections S1, S2, S3 and S4. The average flux of each section is estimated by VFLUX using the measured temperatures at the four sections. A negative flux indicates upward flow, and a positive flux indicates downward flow. Figure **b** shows the measured versus simulated flows for the Zhongtian River. Figure **c** is the boxplot of the GW-SW exchange volume. The red box represents the data in the middle of the upper and lower quartiles. The middle line in the box represents the median, and the small box in the middle represents the average

in the observation period, the surface water in the three downstream sections returned water to the subsurface and supplied groundwater.

4.2 Estimation of the Interaction between GW and SW

The measured water level data were used to calibrate the model parameters in the PSO optimal algorithm, and flood routing was simulated by the three MC methods that could estimate the exchange between GW and SW (MCL1, NMCL1, and NMCL2).

Figure 4b shows that all three MC methods can successfully simulate the outflow, while the NMCL2 method provides the best fit, with a resultant SSQ walue of 0.014, an NSE value of 0.99, and RMSE values as small as 0.008.

The GW-SW exchanges estimated by MCL1 and NMCL1 were similar at the starting point with values of ~0 m^3/s, and the results were negative throughout the whole simulation period. The results revealed that in the MCL1 and NMCL1 methods, during the whole simulation period, the flow was downward due to the GW-SW exchange. The results simulated by NMCL2 were positive at the beginning and converted from positive to negative close to the starting point of the flow rise. This shows that the rising streamflow caused by rainfall resulted in an increase in the downward groundwater recharge.

Figure 4c is a boxplot showing the GW-SW exchanges calculated by MCL1, NMCL2, and NMCL1. The MCL1 and NMCL1 methods provided all negative results, and the results of MCL1 were larger than those of NMCL1. The simulation results of the MCL1 method were much larger than those of NMCL1. Among the three methods, the results of the NMCL1 method had the narrowest distribution, while the result of the MCL1 method had the broadest distribution. Figure 4a shows that the vertical flux direction of the four sections changed during the observation period; this result proves that the GW-SW exchange did exist, and the amount of water supplied by groundwater was smaller than the loss of surface water. According to Fig. 4b, c, the amount of surface water gained from the groundwater and lateral inflow was slightly greater than the amount of water lost. With a rise in the river water level, the exchange volume gradient changed, and the simulation results became negative, indicating that the surface water mainly lost water. The trends of the simulation results of the two methods were consistent. Compared with the thermal-based method, the flood routing method proposed by this study is more accurate, easier to operate, and can simulate overall changes in the GW-SW exchange volumes. When a field investigation is limited, more reliable dynamic flood routing data can be obtained by numerical simulations. In addition, before the field survey, the numerical simulation method can also be used to predict the flow routing to make the field work more feasible.

5 Discussion

5.1 Parameter Estimations Affected by the Type of Model and Flood

There have been many discussions in the literature on optimal parameter estimation methods (Kang et al. 2017; Karahan et al. 2015), but there is a lack of discussion on the influence of parameter change on model results. Six methods were compared in this study, and some parameters used in different methods have the same meaning. However, in simulations of the same flood, the optimal results obtained for parameters with the same meaning are distinct among different methods. In the four historical flood cases simulated in this paper, it can be found that the optimal results of x and K in different methods are quite different for floods with large lateral inflows, e.g., O'Donnell 1985. The parameters K and $x$are determined according to the channel and flood characteristics. Therefore, it is thought that a river channel with obvious lateral inflow cannot be calculated according to the ordinary formula. The parameter x is a weighting factor between the inflow and outflow and represents the degree of flattening during flood wave propagation (Yang et al. 2019). The storage capacity in rivers with large lateral inflows should not be simply divided into inflows and outflows; thus, the expression formula and range of $x$should be reconsidered. The parameter K represents the time required to cover the basin space in each time interval (Gsiorowski and Szymkiewicz 2020). However, the confluence speed of lateral inflow is often much slower than that of normal surface confluence, so the method used to calculate K should also be reconsidered. The parameter calculation method for a channel with large lateral inflow needs to be further studied.

5.2 Limitation and Perspective

In this study, the results of the improved Muskingum-Cunge method and the temperature tracing method are compared to prove the reliability of the improved method in estimating the

GW-SW exchange. However, it is worth noting that there many restrictions exist when estimating the exchange between GW and SW. Although the temperature tracing method can reveal a change in the flux, there is a large error in the quantity estimation.

In the future, we will carry out comparative analyses of the hydro-chemical method and the watershed hydrological simulation method for the test site to better illustrate the applicability of the improved MC method and combine the method with groundwater flood early warning systems (Gotkowitz et al. 2014; Hughes et al. 2011) to prevent flood hazards.

6 Conclusions

The Muskingum method has been widely used because of its simplicity. Whether in the linear or nonlinear Muskingum model, the accuracy of the simulation results completely depends, to a certain extent, on the choice of parameters. Although many studies have been published on the methods used to obtained optimal parameters, the analysis of these parameters often complicates the simulations, negating the simplification of the Muskingum model. In this study, through a parameter sensitivity analysis, the high-sensitivity parameters and low-sensitivity parameters were distinguished. For highly sensitive parameters, parameter estimations are needed before simulations can be conducted, while for parameters with low sensitivities, empirical values can be selected according to the range of parameter analysis results.

River floods are often accompanied by groundwater and surface water exchanges that cannot be ignored. During heavy rainfall, the groundwater level and discharge may increase sharply, far beyond the normal values, and these increases may lead to inundation of the nearby ground. In this paper, the improved MC method is used to simulate flood routing and estimate the groundwater and surface water exchange. The accuracy of the model is verified by three historical datasets and a measured case. The improved model can prevent groundwater flooding in extreme flood events and has practical significance in groundwater management and flood control.

Acknowledgements All authors except Y.Z. were supported by the National Key R&D Program of China (2018YFC0407701), Fundamental Research Funds for the Central Universities (B200202025), National Natural Science Foundation of China (41971027), and Natural Science Foundation of Jiangsu (BK20181035).

Data Availability Not applicable.

Code availability Not applicable.

Author Contributions CL: Conceptualization, Methodology, Supervision, Writing-Reviewing and Editing, Funding acquisition. KJ: Software, Formal analysis, Writing - Original Draft. WW: Validation, Writing - Reviewing and Editing. YZ: Validation, Writing - Reviewing and Editing. TKE: Writing - Review & Editing. WQ: Formal analysis, Visualization. JL: Formal analysis, BL: Investigation, Projection administration, LS: Conceptualization, Funding acquisition.

Declarations

Ethical Approval Not applicable.

Consent to Participate Not applicable.

Consent to Publish Not applicable.

Conflict of Interest The authors declare that they has no competing interests.

References

Ahiablame L, Chaubey I, Engel B, Cherkauer K, Merwade V (2013) Estimation of annual baseflow at ungauged sites in Indiana USA. J Hydrol 476:13–27

Ayvaz MT, Gurarslan G (2017) A new partitioning approach for nonlinear Muskingum flood routing models with lateral flow contribution. J Hydrol 553:142–159

Barbetta S, Moramarco T, Perumal M (2017) A Muskingum-based methodology for river discharge estimation and rating curve development under significant lateral inflow conditions. J Hydrol 554:216–232

Cunge JA (1969) On the subject of a flood propagation computation method (Muskingum method). J Hydraul Res 7:205–230

Doherty J (2004) PEST model-independent parameter estimation users manual. Watermark Numerical Computing, Brisbane, Australia

Eberhart R, Kennedy J (1995) A new optimizer using particle swarm theory. In: Proceedings of the Sixth International Symposium on Micro Machine and Human Science. Nagoya, Japan, pp 39–43

Geem ZW (2006) Parameter estimation for the nonlinear Muskingum model using the BFGS technique. J Irrig Drain Eng 132:474–478

Gill MA (1978) Flood routing by the Muskingum method. J Hydrol 36:353–363

Gotkowitz MB, Attig JW, McDermott T (2014) Groundwater flood of a river terrace in Southwest Wisconsin, USA. Hydrogeol J 22(6):1421–1432

Gsiorowski D, Szymkiewicz R (2020) Identification of parameters influencing the accuracy of the solution of the nonlinear muskingum equation. Water Resour Manag 11

Hatch CE, Fisher AT, Revenaugh JS, Constantz J, Ruehl C (2006) Quantifying surface water-groundwater interactions using time series analysis of streambed thermal records: method development. Water Resour Res 42(10):W10410

Hughes AG, Vounaki T, Peach DW, Ireson AM, Jackson CR, Butler AP, Bloomfield JP, Finch J, Wheater HS (2011) Flood risk from groundwater: examples from a chalk catchment in southern England. J Flood Risk Manag 4(3):143–155

Hussein M, Schwartz FW (2003) Modeling of flow and contaminant transport in coupled stream–aquifer systems. J Contam Hydrol 65(1–2):41–64

Kabala ZJ (2001) Sensitivity analysis of a pumping test on a well with wellbore storage and skin. Adv Water Resour 24(5):483–504

Kang L, Zhou LW, Zhang S (2017) Parameter estimation of two improved nonlinear Muskingum models considering the lateral flow using a hybrid algorithm. Water Resour Manag 31(14):4449–4467

Karahan H (2012) Predicting Muskingum flood routing parameters using spreadsheets. Comput Appl Eng Educ 20(2):280–286

Karahan H, Gurarslan G, Geem ZW (2013) Parameter estimation of the nonlinear Muskingum flood-routing model using a hybrid harmony search algorithm. J Hydrol Eng 18(3):352–360

Karahan H, Gurarslan G, Geem ZW (2015) A new nonlinear Muskingum flood routing model incorporating lateral flow. Eng Optimiz 47:737–749

Krause S, Hannah DM, Fleckenstein JH, Heppell CM, Kaeser D, Pickup R, Pinay G, Robertson AL, Wood PJ (2011) Inter-disciplinary perspectives on processes in the hyporheic zone. Ecohydrology 4:481–499

Lu C, Ji K, Zhang Y, Fleckenstein JH, Zheng C, Salsky K (2020) Event-driven hyporheic exchange during single and seasonal rainfall in a gaining stream. Water Resour Manag 34:4617–4631

Moghaddam A, Behmanesh J, Farsijani A (2016) Parameters estimation for the new four-parameter nonlinear Muskingum model using the particle swarm optimization. Water Resour Manag 30(7):2143–2160

Mohan S (1997) Parameter estimation of nonlinear muskingum models using genetic algorithm. J Hydraul Eng-Asce 123(2):137–142

Moon SK, Woo NC, Lee KS (2004) Statistical analysis of hydrographs and water-table fluctuation to estimate groundwater recharge. J Hydrol 292:198–209

Niazkar M, Afzali SH (2015) Assessment of modified honey bee mating optimization for parameter estimation of nonlinear Muskingum models. J Hydrol Eng 23(4):04014055

O'Donnell T (1985) A direct three-parameter Muskingum procedure incorporating lateral inflow. Hydrol Sci J 30:479–496
Schmidt C, Bayer-Raich M, Schirmer M (2006) Characterization of spatial heterogeneity of groundwater-stream water interactions using multiple depth streambed temperature measurements at the reach scale. Hydrol Earth Syst Sci 3(6):1419–1446
Shuai P, Cardenas MB, Knappett PSK, Bennett PC, Neilson BT (2017) Denitrification in the banks of fluctuating rivers: the effects of river stage amplitude, sediment hydraulic conductivity and dispersivity, and ambient groundwater flow. Water Resour Res 53(9):7951–7967
Tran QD, Ni CF, Lee IH, Truong MH, Liu CJ (2020) Numerical modeling of surface water and groundwater interactions induced by complex fluvial landforms and human activities in the pingtung plain groundwater basin, Taiwan. Appl Sci-Basel 10:7152
Tung YK (1985) River flood routing by nonlinear Muskingum method. J Hydraul Eng-ASCE 111(12):1447–1460
Viessman W, Lewis GL (2003) Introduction to hydrology. Prentice Hall India (P) limited, New Jersey
Welch C, Cook PG, Harrington GA, Robinson NI (2013) Propagation of solutes and pressure into aquifers following river stage rise. Water Resour Res 49(9):5246–5259
Werner AD, Gallagher MR, Weeks SW (2006) Regional-scale, fully coupled modelling of stream-aquifer interaction in a tropical catchment. J Hydrol 328(3–4):497–510
Wilson EM (1974) Engineering hydrology. Wiley, New York
Yang W, Wang J, Sui J, Zhang F, Zhang B (2019) A modified muskingum flow routing model for flood wave propagation during river ice thawing-breakup period. Water Resour Manag 33(2):4865–4878

Publisher's Note Springer Nature remains neutral with regard to jurisdictional claims in published maps and institutional affiliations.

Affiliations

Chengpeng Lu[1] · Keyan Ji[1] · Wanjie Wang[1] · Yong Zhang[2] · Tema Koketso Ealotswe[1] · Wei Qin[1] · Jiayun Lu[1] · Bo Liu[1] · Longcang Shu[1]

[1] College of Hydrology and Water Resources, Hohai University, Nanjing 210098 Jiangsu, China

[2] Department of Geological Sciences, University of Alabama, Tuscaloosa, AL 35487, USA